Influence of the Preparation Procedure on the Catalytic Activity of Gold Supported on Diamond Nanoparticles for Phenol Peroxidation

ARTICLE *in* CHEMISTRY - A EUROPEAN JOURNAL · AUGUST 2011

Impact Factor: 5.73 · DOI: 10.1002/chem.201100955 · Source: PubMed

6 AUTHORS, INCLUDING:

Juan José Delgado
Universidad de Cádiz
91 PUBLICATIONS **1,708** CITATIONS
SEE PROFILE

Jose J Calvino
Universidad de Cádiz
173 PUBLICATIONS **3,398** CITATIONS
SEE PROFILE

Mercedes Alvaro
Universitat Politècnica de València
215 PUBLICATIONS **5,409** CITATIONS
SEE PROFILE

Hermenegildo Garcia
Technical University of Valencia
631 PUBLICATIONS **21,924** CITATIONS
SEE PROFILE

CHEMISTRY
A EUROPEAN JOURNAL

DOI: 10.1002/chem.201100955

Influence of the Preparation Procedure on the Catalytic Activity of Gold Supported on Diamond Nanoparticles for Phenol Peroxidation

Roberto Martin,[a] Sergio Navalon,[a] Juan Jose Delgado,[b] Jose J. Calvino,[b] Mercedes Alvaro,[a] and Hermenegildo Garcia*[a]

Abstract: The catalytic activity of diamond-supported gold nanoparticle (Au/D) samples prepared by the deposition/precipitation method have been correlated as a function of the pH and the reduction treatment. It was found that the most active material is the one prepared at pH 5 followed by subsequent thermal treatment at 300 °C under hydrogen. TEM images show that Au/D prepared under optimal conditions contain very small gold nanoparticles with sizes below 2 nm that are proposed to be responsible for the catalytic activity. Tests of productivity using large phenol (50 g L^{-1}) and H_2O_2 excesses (100 g L^{-1}) and reuse gives a minimum TON of 458,759 moles of phenol degraded per gold atom. Analysis of the organic compounds extracted from the deactivated solid catalyst indicates that the poisons are mostly hydroxylated dicarboxylic acids arising from the degradative oxidation of the phenyl ring. By determining the efficiency for phenol degradation and the amount of O_2 evolved two different reactions of H_2O_2 decomposition (the Fenton reaction at acidic pH values and spurious O_2 evolution at basic pH values) are proposed for Au/D catalysis. The activation energy of the two processes is very similar (ranging between 30 and 35 kJ mol^{-1}). By using dimethylsulfoxide as a radical scavenger and *N*-*tert*-butyl-α-phenylnitrone as a spin trap under aerated conditions, the EPR spectrum of the expected PBN–OCH_3 adduct was detected, supporting the generation of HO•, characteristic of Fenton chemistry in the process. Phenol degradation, on the other hand, exhibits the same activation energy as H_2O_2 decomposition at pH 4 (due to the barrierless attack of HO• to phenol), but increases the activation energy gradually up to about 90 kJ mol^{-1} at pH 7 and then undergoes a subsequent reduction as the pH increases reaching another minimum at pH 8.5 (49 kJ mol^{-1}).

Keywords: diamond · gold · heterogeneous catalysis · nanoparticles · transmission electron microscopy

Introduction

The Fenton reaction consists of the stoichiometric reduction of H_2O_2 by Fe^{2+} salts at acidic pH leading to the generation of hydroxyl radicals (HO•) [Eq. (1)].[1–3] The main use of the Fenton reaction is the degradation of organic pollutants in aqueous solutions caused by the attack of highly reactive HO•. Besides Fe^{2+} salts other transition-metal ions, such as Cu^{2+}, Mn^{2+}, Ru^{2+}, and Ce^{2+}, can also be used to effect the reduction of H_2O_2.[4] The main limitations of the Fenton reaction hampering their wide use for pollution remediation are the need of stoichiometric amounts of Fe^{2+} salts and large excesses of H_2O_2. Therefore, there is a great interest in developing catalytic processes in which H_2O_2, acting simultaneously as an oxidizing and reducing agent, forms HO• without the need of equivalent amounts of transition metals. In addition, the spurious decomposition of H_2O_2 to H_2O and O_2 should be minimized as much as possible. Partial success in developing catalytic versions of the Fenton reaction have been reported by using Fe-containing aluminosilicates, such as zeolites and layered clays.[4] By using these metal-containing solids as heterogeneous catalysts, the Fenton reaction can proceed under large excesses of H_2O_2 at acid pH values or even at neutral pH increasing the reaction temperature.

Related to the present work is a recent report in which gold nanoparticles supported on hydroxyapatite act as a heterogeneous catalyst for the Fenton degradation of phenol at moderate temperatures.[5] In this report, however, a large of excess H_2O_2 with respect to phenol (about 400 equivalents) was used. Considering that H_2O_2 is a relatively costly commodity and that for environmental applications it is necessary to optimize the amount of H_2O_2 used as much as possible, it would be still desirable to develop more efficient catalysts. In this context, we have recently reported that gold nanoparticles supported on Fenton-treated diamond nanoparticles (Au/D) is an extremely efficient solid catalyst for the

[a] Dr. R. Martin, Dr. S. Navalon, Prof. M. Alvaro, Prof. H. Garcia
Instituto de Tecnología Química CSIC-UPV and
Departamento de Química
Universidad Politécnica de Valencia
Av. De los Naranjos s/n, 46022 Valencia (Spain)
Fax: (+34) 963-877-809
E-mail: hgarcia@quim.upv.es

[b] Dr. J. J. Delgado, Dr. J. J. Calvino
Departamento de Ciencia de Materiales e Ingeniería
Metalúrgica y Química Inorgánica
Facultad de Ciencias, Universidad de Cádiz.
Campus Río San Pedro, 11510 Puerto Real, Cádiz (Spain)

Supporting information for this article is available on the WWW under http://dx.doi.org/10.1002/chem.201100955.

process using quasi-stoichiometric amounts of H_2O_2 with respect to phenol.[6] The preliminary data has shown that at least 79% of H_2O_2 is converted into HO•.[6] Furthermore, in the absence of phenol, H_2O_2 decomposition promoted by Au/D is very slow while in the presence of phenol no oxygen formation is observed, which indicates that dismutation of H_2O_2 is not taking place. Also, the reported TON of phenol degradation by using Au/D was 321,000.

Based on these precedents and considering the unique catalytic activity of Au/D it is of interest to undertake a comprehensive study addressing the optimal preparation conditions to achieve the highest catalytic activity and to gain further insight into the nature of the active sites, the reaction mechanism, and the catalytic stability of the material. In the present work, we have studied the catalytic activity of a series of Au/D samples obtained by different preparation procedures to determine the influence of these parameters on the catalytic activity and report a reliable preparation procedure. High-resolution transmission electron microscopy (HRTEM) has been used to correlate the catalytic activity of Au/D for Fenton chemistry with the particle size and the number of external gold atoms.

Results and Discussion

Catalysts characterization: Preparation of Au/D catalysts consists in the formation of gold nanoparticles on the surface of Fenton-treated diamond nanoparticles (D). It has been already shown that Fenton treatment is necessary to obtain adequate D samples suitable for being used as gold supports.[6] On one hand, Fenton treatment of commercial D significantly decreases the presence of amorphous carbon that is present in the commercial D samples prepared by the detonation method.[7] On the other hand, Fenton treatment introduces surface hydroxy groups on D that are later necessary for the deposition/precipitation of gold. Finally, the Fenton treatment makes even more inert the surface of diamond, a characteristic that is beneficial to increase the proportion of free HO• available for the reaction.

By using Fenton-treated D as a support gold nanoparticles are formed by following the deposition/precipitation method.[8,9] In this procedure an aqueous solution of $HAuCl_4$ at the appropriate pH value is contacted with the support and the suspension is left for a sufficiently long period (for instance 48 h) to effect the anchoring of gold species on the solid surface. After that, nucleation and particle growth is effected by reducing Au^{3+} with a suitable reducing agent. The key parameters of the deposition/precipitation method are the pH value of the suspension during the deposition step and the reduction procedure in the precipitation step.[8] In the case of metal oxides, such as TiO_2 and CeO_2, it has been found that the pH of the deposition in the range 4 to 10 controls the yield of gold adsorption on the solid (the percentage of the Au present in the solution that becomes deposited onto the support) and also the particle size of gold in the resulting samples.[10] These parameters are interconnected and are known to exert a strong influence on the catalytic activity of gold nanoparticles. Considering these precedents in the present work we have prepared a series of samples in which the pH of the deposition was fixed to 5, 7.5, or 10.

Also with respect to the nucleation and particle formation, typical reducing agents that have been used are alcohols, thermal treatment with hydrogen flow gas, and metal hydride.[11] In some precedents in gold catalysis it has been found that the actual reduction procedure can play an important role determining the catalytic activity, whereas in other reports the relevance of the reduction procedure was marginal.[12] Therefore, the influence of the reduction procedure on the activity of Au/D cannot be anticipated from the literature.

The list of Au/D samples prepared in the present study, the preparation procedure, and their gold loading are indicated in Table 1. The code for the samples includes a number corresponding to the pH of the deposition and a letter that indicates the reducing agent (B: $NaBH_4$, H: H_2, and P: 1-phenylethanol). The Au content in weight percent of each sample is also indicated in Table 1.

Table 1. Samples and gold content (wt.%) of Au/D catalysts. The numbers outside the brackets indicate the gold loading in weight percentage.

pH[a]	Gold reduction method		
	borohydride	1-phenylethanol	H_2 thermal treatment
5	Au/D (5B) 0.99	Au/D (5P) 0.99	Au/D (5H) 0.99
7.5	Au/D (7.5B) 0.98	Au/D (7.5P) 0.97	Au/D (7.5H) 0.98
10	Au/D (10B) 0.68	Au/D (10P) 0.70	Au/D (10H) 0.71

[a] Refers to the pH of the gold solution during the deposition procedure of $AuCl_4^-$ on Fenton-treated D.

The particle size distribution and morphology of the gold nanoparticles supported on diamond was determined by TEM. All the samples exhibited a wide particle size distribution and the presence of very large gold particles not associated to diamond was observed regardless of the preparation procedure (see Figures S1–S9 in the Supporting Information). We assume that these large gold particles (>15 nm) not associated to D are catalytically not relevant and are formed by agglomeration of gold crystallites not anchored to the solid support. In addition, TEM also reveals that except for the samples prepared at pH 10, the rest of the Au/D samples contain small gold particles of a size below 5 nm with cuboctahedric morphology (see Figures S1–S9 in the Supporting Information). A large population of these small gold nanoparticles were present in those samples prepared by hydrogen or 1-phenylethanol reduction when the deposition was carried out at pH 5 or 7.5. Table 2 summarizes the average particle size distribution and the fraction of gold surface atoms as a function of the preparation procedure.

To illustrate the differences in the average particle size, Figure 1 shows a representative HRTEM of Au/D (5H) compared to selected images of Au/D (5B) and Au/D

Table 2. Average particle size distribution and surface gold atoms (indicated in brackets) as a function of the preparation method.[a]

pH[b]	Gold reduction method		
	borohydride	1-phenylethanol	H_2 thermal treatment
	particles smaller than 5 nm		
5	2.5 (42%)	1.0 (73%)	0.9 (75%)
7.5	2.4 (48%)	1.3 (58%)	0.8 (79%)
10	_[c]	_[c]	_[c]
	complete collection of particles		
5	12.3 (6.2%)	7.9 (12.2%)	7.7 (12.4%)
7.5	13.0 (7.5%)	9.3 (9.8%)	8.6 (11.6%)
10	9.4 (11.0%)	14.2 (8.0%)	13.9 (7.3%)

[a] Estimation of the fraction of gold atoms exposed on the surface was made assuming a predominant cuboctahedric morphology and determining the average particle size as indicated in Equation (4) of the Experimental Section. [b] pH value during the gold deposition step on D. [c] Nanoparticles below 5 nm were not observed.

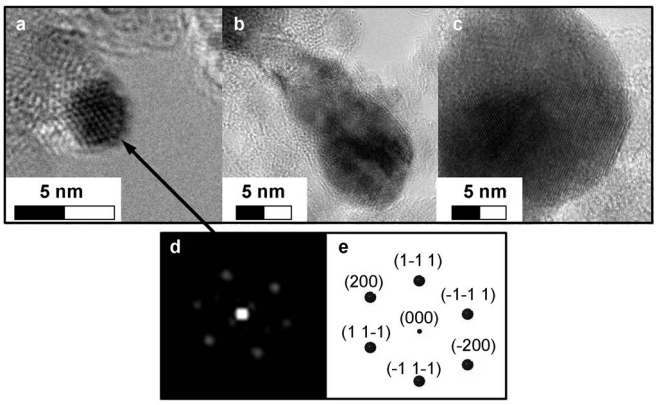

Figure 1. Selected HRTEM images of Au/D samples: a) Au/D (5H); b) Au/D (5B); c) Au/D (10H); d) digital diffraction pattern (DDP) of the particle shown in a), which corresponds to the face-centered cubic structure of gold in a [110] direction; e) Kinematic simulation of the DDP.

(10H). As can be seen in these selected images, the gold particle size is very different depending on the deposition pH and the gold reduction method. The outcome of this TEM study is that Au/D (5H) and Au/D (5P) contain a large population of gold nanoparticles below 1.5 nm. As will be commented on later the presence of these small gold particles can be correlated with the catalytic activity of the samples.

After the Fenton treatment, D undergoes a significant increase in the population of hydroxyl groups as determined by the corresponding FTIR spectrum of D samples.[6,13,14] In supported gold catalysts it is well-known that deposition of gold is due to the covalent anchoring of gold species (such as $AuCl_4^-$) on the surface hydroxyl groups of the support.[11] Therefore FTIR spectroscopy could be a suitable technique to follow the changes in the functional groups and, particularly the evolution of hydroxyl groups. Figure 2 presents the FTIR spectra of some of the samples prepared to illustrate the changes occurring upon deposition of Au nanoparticles on D. As a general trend, the nine samples exhibited a significantly reduced intensity of the −O−H vibration band relative to that of the initial Fenton treated D. This can be estimated quantitatively by determining the intensity area corresponding to hydroxyl groups. A full set of FTIR spectra can be found in Figures S10 and S12 in the Supporting Information.

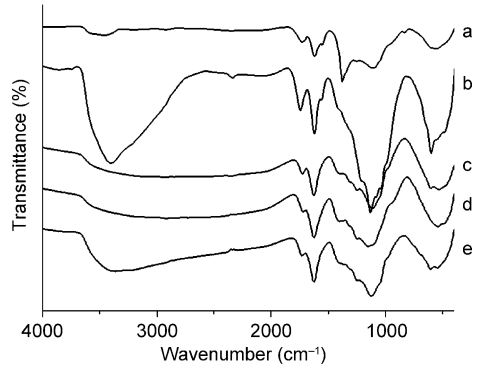

Figure 2. FTIR spectra of commercial D (a), Fenton-treated D (b) and samples Au/D (5H) (c), Au/D (5B) (d), and Au/D (5P) (e).

Powder XRD diffraction of the samples show in all cases the expected pattern for diamond accompanied by the three peaks corresponding to gold. As an example, Figure 3 shows

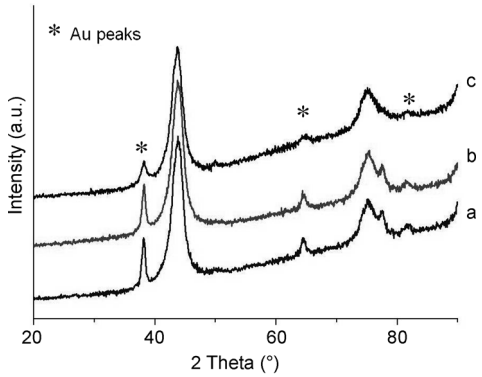

Figure 3. Powder XRD of samples Au/D (5H) (a), Au/D (7.5H) (b), and Au/D (10H) (c); the peaks corresponding to gold have been marked with an asterisk for clarity.

the XRD patterns of selected samples and a full set of XRD are provided in the Supporting Information (see Figures S12 and S13). As can be seen in Figure 3, it is remarkable that gold, even at very low loadings, as those indicated in Table 1, exhibits a clear diffraction pattern. This can be due to the much higher atomic mass of gold relative to carbon that would apparently enhance diffraction of the metal with respect to diamond. In addition, we have not found significant differences in full width at half height of the bands corresponding to gold depending on the sample preparation. This can be due to the presence in all cases of a population of large gold particles that are presumably the ones that contribute to a larger extent to the observed diffraction pattern.

Optical spectroscopy of the samples reveals the presence of gold nanoparticles by observing the characteristic gold surface plasmon band at about 540 nm (see Figures S14–S16

in the Supporting Information). This band appears on top of the broad background due to D that generally appears as grey solids absorbing in the whole range of the UV/Vis region, but without a defined peak.

Catalytic activity

Phenol degradation and H_2O_2 decomposition by using Au/D catalysts: The main purpose of this work is to assess the influence of the preparation procedure on the catalytic activity for the Fenton reaction of diamond-supported gold nanoparticles and to provide a reliable protocol for their preparation.

To determine the catalytic activity of the nine samples, we selected the reported optimum conditions for phenol degradation and followed the temporal profiles of phenol disappearance and H_2O_2 decomposition in the presence of the diamond-supported gold catalysts. HPLC analysis of the reaction mixtures indicates that the primary aromatic products arising from the Fenton treatment of phenol are hydroquinone, benzoquinone, and catechol. A summary of the results

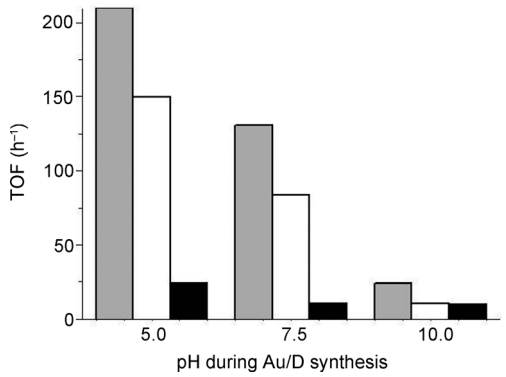

Figure 4. TOF for the different Au/D catalysts determined at 50% phenol degradation. TOF has been estimated by considering the number of phenol molecules degraded (mM) per gold atoms (mM) in the required time to achieve 50% phenol degradation. ■: H_2 thermal treatment, □: 1-phenylethanol, ■: borohydride.

given as turnover frequency values (TOF) measured at 50% of degraded phenol are presented in Figure 4.

As can be seen from Figure 4, there is a considerable influence of the preparation procedure on the catalytic activity, the best sample being the Au/D that was prepared by hydrogen reduction after deposition of gold at pH 5. Figure 5 shows the time conversion plot for phenol disappearance for the three Au/D samples prepared by thermal reduction with H_2. From the data of TOF shown in Figure 4, it can be concluded that both the reduction method used in the final step of sample preparation and the pH of the deposition step control the catalytic activity. In general, reduction with sodium borohydride or by boiling the solid in 1-phenylethanol after deposition of gold at pH values higher than 5 appear much less adequate than reduction by thermal treatment with hydrogen at 300 °C. Also, the pH of the deposition plays a role in the catalytic activity, the most active Au/D solids being those in which the gold has been deposited at lower pH values. This influence of the deposition pH on the catalytic activity is most probably due to the differences in the particle size of gold nanoparticles as a function of the gold loading and particle size. According to Table 2, the proportion of the gold atoms at the external surface exposed to the substrate decreases as the pH of the deposition increases. The linear relationship between the initial phenol reaction rate and the percentage of surface gold atoms indicates that all the gold atoms at the surface are equally active (see Figure S17 in the Supporting Information). Therefore, the key parameter of the catalytic activity is to achieve a large surface area for supported gold nanoparticles.

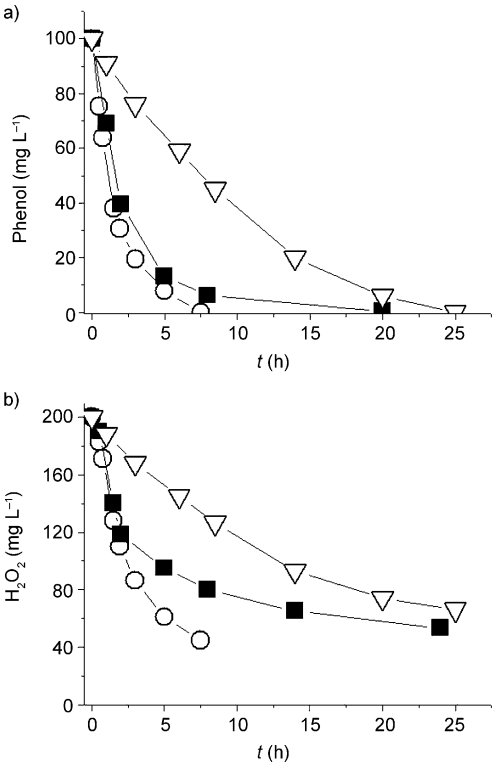

Figure 5. Phenol degradation (a) and H_2O_2 decomposition (b) in the presence of Au/D catalysts; ○: Au/D (5H), ■: Au/D (7.5H), ▽: Au/D (10H). Reaction conditions: phenol (100 mg L^{-1}, 1.06 mM), H_2O_2 (200 mg L^{-1}, 5.88 mM), Au (0.005 mM), pH 4, room temperature.

The occurrence of leaching of gold species from the Au/D catalysts to the aqueous phase was determined by ICP-AES

Table 3. Percentage of leached gold (at 24 h) for the different Au/D catalysts. Reaction conditions: phenol (100 mg L^{-1}), H_2O_2 (200 mg L^{-1}), pH 4, 0.005 mM Au catalyst, RT, 24 h.

pH[a]	Gold reduction method		
	borohydride	1-phenylethanol	H_2 thermal treatment
5	9.1	<LOD[b]	<LOD
7.5	3.2	<LOD	<LOD
10	0.08	<LOD	<LOD

[a] pH during the deposition step of $AuCl_4^-$ on Fenton-treated diamond nanoparticles. [b] LOD: limit of detection.

analysis of the solution after the Fenton reaction at pH 4. The analytical results are listed in Table 3 and show that for the most active Au/D samples the Au content was lower than the detection limit (0.1 $\mu g L^{-1}$).

Temperature and pH effect of Au/D (5H) on phenol degradation and H_2O_2 decomposition: After having determined the best preparation procedure, we have studied the influence on the catalytic activity of Au/D (5H) for the Fenton reaction of the pH and temperature. Previously, we have already shown that the catalytic activity of Au/D is strongly influenced by the reaction conditions, the optimal pH being in the window of 3.5–4.5.[6] This study was carried out at room temperature. In Fenton chemistry the remarkable influence of the reaction pH is well established.[4] Also, in the field of heterogeneous catalysis for the Fenton reaction it is very common to overcome the limitation influence of acid pH requirements by increasing the reaction temperature.[4,15]

Herein by using Au/D (5H) we have carried out a series of experiments by varying the pH from 4 to 10 in the range of temperatures from 20 to 100 °C. The catalytic results considering the initial reaction rate of phenol disappearance and H_2O_2 decomposition are presented in Figure 6.

The linear relationship between the natural logarithm of the initial reaction rate either for phenol disappearance or for H_2O_2 decomposition indicates that the Arrhenius law is obeyed. From this linear correlation, the corresponding activation energy (E_a) for each of the two processes (phenol disappearance and H_2O_2 decomposition) could be determined.

Figure 7 shows the apparent activation energies (E_a) determined from the influence of the temperature on the initial reaction rate. As can be seen in Figure 7, corresponding to the activation energies, H_2O_2 decomposition exhibits similar activation energies (from 30 to 35 $kJ mol^{-1}$) in the pH range under study. Interestingly, the E_a value at pH 4 for the most active sample prepared herein (Au/D (5H)) is 30 $kJ mol^{-1}$, which is significantly lower than the E_a value of the nonoptimized Au/D catalyst previously reported in the literature that was 46 $kJ mol^{-1}$.[15] This difference in E_a values reflects quantitatively the different catalytic activity between Au/D (5H) and the catalyst reported in the literature.[15] This difference in E_a values originates from the variation in the pH of the deposition step and must be ascribed to the different catalytic activity depending on the average size and other characteristics of the gold nanoparticles.

To gain some understanding on the reasons why the activation energy for H_2O_2 decomposition has a small variation over the pH range in spite of the fact that there is a large influence of the pH value on the Fenton reaction, we analyzed the oxygen evolved from H_2O_2 in the presence of phenol by using Au/D (5H) as the catalyst. The results are presented

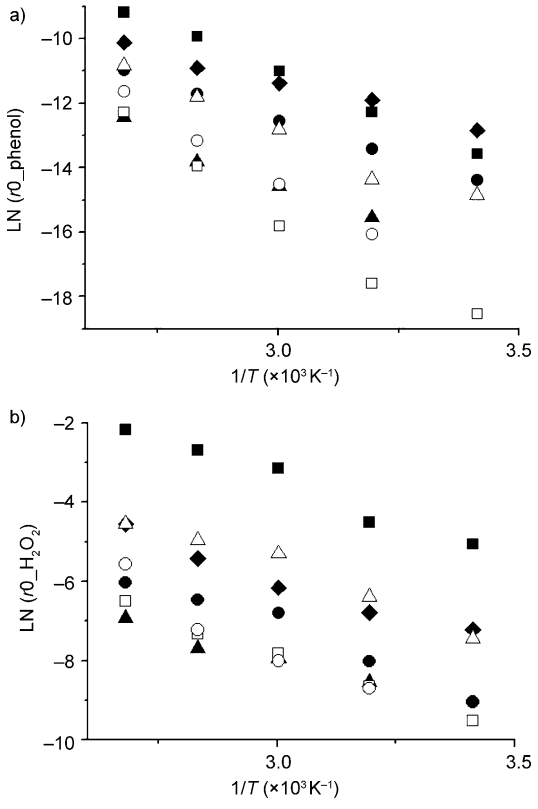

Figure 6. Arrhenius plot for phenol degradation (a) and H_2O_2 decomposition (b). Reaction conditions: phenol (100 $mg L^{-1}$, 1.06 mM); H_2O_2 (200 $mg L^{-1}$, 5.88 mM), catalyst (100 $mg L^{-1}$, 0.005 mM as Au), pH and temperature as indicated in the plot. ◆: pH 4; ●: pH 5.5; ▲: pH 6.5; □: pH 7.0; ○: pH 7.5; △: pH 8.5; ■: pH 10.

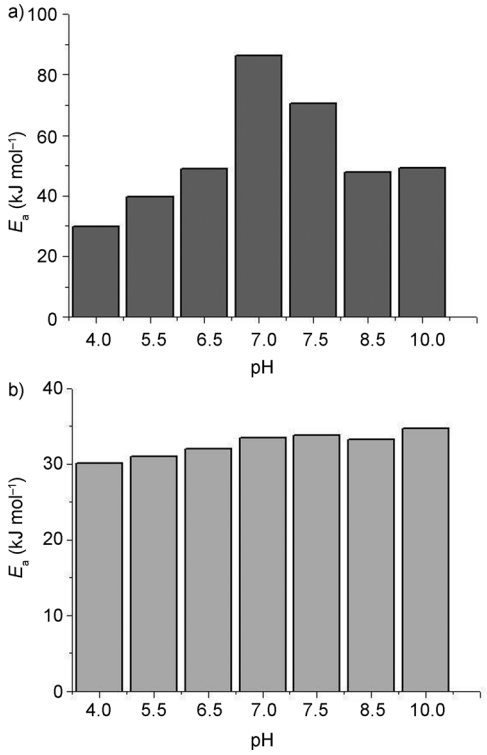

Figure 7. Activation energies for phenol degradation (a) and H_2O_2 decompositon (b). Reaction conditions: phenol (100 $mg L^{-1}$, 1.06 mM); H_2O_2 (200 $mg L^{-1}$, 5.88 mM), Au/D (5H) catalyst (100 $mg L^{-1}$, 0.005 mM as Au), temperature (from 20 to 100 °C) and pH as indicated.

Table 4. Influence of the pH solution value during phenol degradation in the presence of Au/D (5H) catalyst and H_2O_2. Reaction conditions: phenol (100 mg L^{-1}, 1.06 mM), H_2O_2 (200 mg L^{-1}, 5.88 mM), catalyst (100 mg L^{-1}, 0.005 mM as Au), room temperature, 33 h reaction time.

pH	Consumed H_2O_2/ phenol molar ratio	Degraded phenol [%]	Decomposed H_2O_2 [%]	Percentage of evolved O_2 [%]
4[a]	3.8[a]	100[a]	75[a]	0[a]
5.5	4.7	92	78	15
6.5	21	8	30	81
7.0	22	5	20	82
7.5	30	7	49	86
8.5	42	9	70	90
10	79	7	100	95

[a] Obtained results at 8 h reaction time.

in Table 4 in which the percentage of phenol disappearance has also been included for comparison. From the data shown in Table 4 it can be seen that H_2O_2 decomposes to give oxygen at basic pH values in a very large extent, whereas at pH values below 7 oxygen evolution is remarkably lower. In contrast, phenol disappearance reaches the maximum value at acid pH when the amount of oxygen is negligible. From the different pH profiles of phenol disappearance and O_2 evolution it can be inferred that H_2O_2 undergoes two different decomposition pathways depending on the solution pH: at acidic pH values the Fenton reaction prevails leading to phenol disappearance, at basic pH values decomposition of H_2O_2 to O_2 prevails, but H_2O_2 decomposition is not accompanied by a significant degradation of phenol.

Considering that H_2O_2 undergoes two different decomposition reactions depending on the pH, the E_a data obtained for the dependence of the initial reaction rate for H_2O_2 decomposition at various temperatures is surprising in the sense that being two different reactions the E_a values are similar varying from 30 to 35 kJ mol^{-1}. As is indicated in Figure 7, one likely explanation is that E_a for the Fenton chemistry increases gradually by about 2 kJ mol^{-1} per pH unit until it overcomes the E_a of the decomposition to O_2 that becomes the favorable process. The E_a of H_2O_2 decomposition to O_2 decreases with the pH approximately the same value (2 kJ mol^{-1} per pH unit). This interpretation agrees with the fact that at pH 4, in which the catalytic efficiency for $HO^{\bullet}$ generation is maximum, the activation energy for H_2O_2 decomposition and phenol degradation coincide, a fact that is compatible with the attack of $HO^{\bullet}$ (from the H_2O_2 decomposition) to phenol being essentially barrierless. On the other hand, as the pH value increases the activation energy for phenol degradation grows and becomes significantly much larger than the activation energy for H_2O_2 decomposition, which suggests that the species that is being generated at these pH values is not $HO^{\bullet}$ but other less reactive oxygen species, such as hydroperoxyl radicals, superoxide anion, or others.

Influence of oxygen on phenol degradation using Au/D (5H) catalyst: One issue of interest in Fenton chemistry is to determine the influence that the presence of oxygen can play on the degradation of the organic components. Since $HO^{\bullet}$ can generate carbon centered radicals, these carbon-centered radicals may be intercepted by O_2 leading to peroxyl radicals that intervene in a chain mechanism degradation. Equations (1) to (3) summarize the possible role of oxygen favoring phenol decomposition.

$$RH + HO^{\bullet} \rightarrow R^{\bullet} + H_2O \quad (1)$$

$$R^{\bullet} + O_2 \rightarrow ROO^{\bullet} \quad (2)$$

$$ROO^{\bullet} + RH \rightarrow ROOH + R^{\bullet} \quad (3)$$

To address this point, we have studied the disappearance of phenol by the Fenton reaction in the presence of Au/D (5H) at pH 4 under a N_2 atmosphere or under air or pure O_2. Time conversion plots showing the variation of phenol concentration versus time are presented in Figure 8. As can

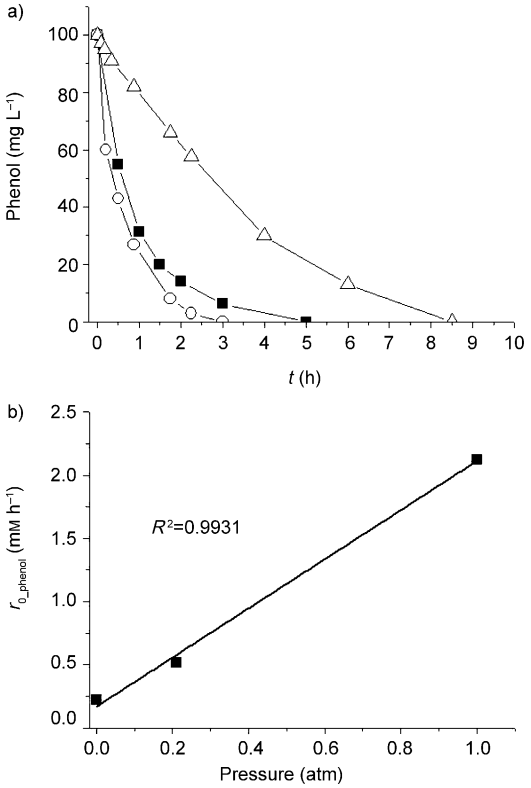

Figure 8. Influence of O_2 on phenol degradation (a) and on the initial reaction rate of phenol disappearance (b). Reaction conditions: phenol (100 mg L^{-1}), H_2O_2 (200 mg L^{-1}), Au/D (5H) catalyst (100 mg L^{-1}, 0.005 mM as Au), pH 4, room temperature. Atmosphere: ■: air, ○: oxygen, △: nitrogen.

be seen in this figure, the presence of O_2 increases the rate of phenol decomposition. Furthermore, a plot of the initial reaction rate for phenol disappearance versus the partial pressure of O_2 shows that the rate constant depends linearly with the O_2 pressure. These results are compatible with the previous Equations (1) and (3) and with the formation of or-

ganic hydroperoxides generated from O_2 being also active to promote phenol disappearance. The favorable influence of O_2 pressure and the linear relationship with O_2 pressure and the initial reaction rate of phenol disappearance are in agreement with other precedents that have already observed that O_2 favors the Fenton reaction.[4,15]

Au/D (H5) catalyst productivity: In heterogeneous catalysis one point of large importance is catalyst deactivation and the maximum productivity of the catalyst.[6] This point was studied by performing the Fenton reaction with a much larger excess of phenol (50 g L^{-1}) and H_2O_2 (100 g L^{-1}) with respect to Au/D (5H) (50 mg L^{-1} catalyst; 0.0025 mM as Au) than in the previous experiments. These reactions were carried out for long reaction times until the catalyst becomes deactivated. At this point the Au/D (5H) catalyst was recovered by filtration, exhaustively washed with basic water (pH 10), and reused for a second consecutive run under the same conditions. Up to four uses of the same Au/D (5H) sample under these conditions of large reagent concentrations with respect to substrate were carried out. The temporal profiles of phenol and H_2O_2 disappearance upon reuse are given in Figure 9. Comparison of this temporal evolution

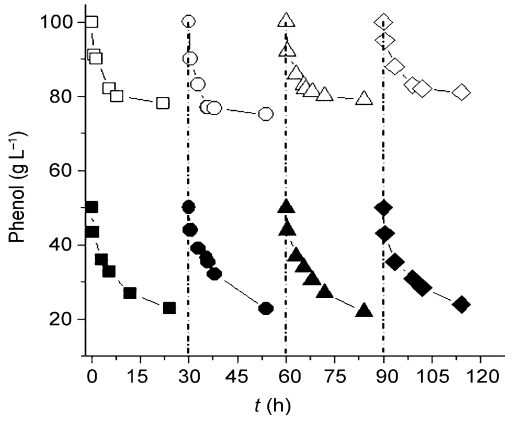

Figure 9. Productivity of Au/D (5H) for phenol decomposition at 50 g L^{-1} (0.53 M) by 100 g L^{-1} H_2O_2 (2.94 M). Reaction conditions: H_2O_2 (5.5 equiv. with respect to phenol), pH 4, room temperature and Au/D (5H) (50 mg L^{-1}, 0.0025 mM Au). H_2O_2: □: 1st use, ○: 2nd use, △: 3rd use, ◇ 4th use; phenol: ■: 1st use, ●: 2nd use, ▲: 3rd use, ◆ 4th use.

shows that not only the final phenol conversion is maintained upon reuse but also that the initial reaction rates and other kinetic parameters are maintained. It can be seen that washing with basic water regenerates the activity of the deactivated catalyst to that of the fresh catalyst. The overall productivity of the four uses was 109.45 g L^{-1} of phenol that corresponds to a minimum TON of 458,759 molecules of phenol degraded per gold atom. It is interesting to comment that when the gold catalyst becomes deactivated, washings with basic water is a simple and suitable reactivation procedure as can be seen in Figure 9.

By analyzing the compounds present in the basic washings a deeper insight into the deactivation mechanism was obtained. Thus, it was observed that the compounds present in the deactivated Au/D and removed with basic water are mostly hydroxylated dicarboxylic acids, such as malic and tartaric acids. The most likely origin of these acids is the oxidative degradation of the benzene ring of phenol as has been reported in related precedents.[15]

Quenching of HO• by DMSO: To confirm the generation of HO• radicals by using Au/D (5H) as a solid catalyst, we performed the decomposition of H_2O_2 in the absence of phenol but in the presence of DMSO as a radical scavenger and PBN as a spin-trap, and followed the process by EPR spectroscopy. It has been reported that HO• reacts with DMSO, producing the decomposition of this sulfoxide, leading to the generation of methyl radicals.[16] These methyl radicals under aerobic conditions can be converted into methoxyl radicals and can be trapped by PBN. PBN will trap the radicals present in the medium forming adducts of sufficiently long lifetime to be characterized by conventional EPR spectroscopy.[16] By performing decomposition of H_2O_2 in the presence of DMSO and PBN, the EPR spectra shown in Figure 10 was recorded. This experimental EPR spectrum agrees well with that of PBN–OCH_3. For the sake of comparison, Figure 10 shows a comparison of the EPR spectrum recorded for the reaction of H_2O_2 in DMSO containing PBN with the simulated spectrum of the PBN–OCH_3 adduct. Considering the coincidence of the fine structure and the hyperfine couplings, the EPR spectrum shown in Figure 10 constitutes a strong piece of evidence supporting the generation of HO• by using H_2O_2 and Au/D as the catalyst.

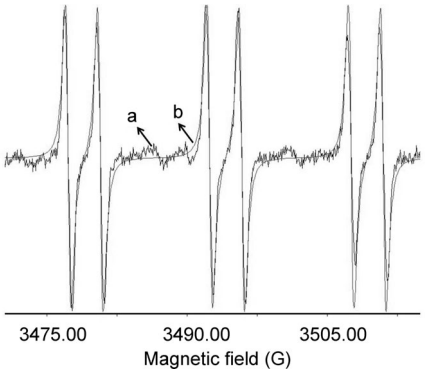

Figure 10. a) Au/D (5H), H_2O_2, PBN, pH 4, DMSO; b) EPR simulation of the adduct of CH_3O• and PBN. Hyperfine coupling constants from CH_3O• adduct by using PBN: $A_N/G = 15.08$; $A_H/G = 3.52$, coinciding with reported values in the literature [16]. Reaction conditions: Au/D (5H) catalyst (100 mg L^{-1}), H_2O_2 (200 mg L^{-1}), PBN/H_2O_2 molar ratio 1, pH 4, DMSO/H_2O_2 molar ratio 10.

Conclusion

In the present work we have shown that the catalytic activity of diamond-supported gold nanoparticles for the Fenton reaction is strongly dependent on the preparation proce-

dure, particularly the pH and the reduction conditions. The most active sample (TON 458,759) is the one obtained by the deposition/precipitation method at pH 5 and subsequent reduction with hydrogen at 300 °C. The influence of the pH and reaction temperature was determined by using the most active Au/D (5H) and the corresponding activation energies estimated from the Arrhenius plot of the initial reaction rate versus the inverse of temperature for phenol disappearance and H_2O_2 decomposition. Based on the influence of the pH on the oxygen evolution, the kinetic data have been interpreted proposing that H_2O_2 undergoes two different decomposition mechanisms depending on the pH of the medium. At acidic pH values, the Fenton reaction (generation of $HO^{\bullet}$ radicals) prevails, whereas at basic pH, decomposition towards oxygen is the process being catalyzed by Au/D. Overall, the data presented indicate that probably due to the inertness of the diamond surface leading to free hydroxyl radicals, Au/D (5H) properly prepared is by several orders of magnitude more efficient (larger proportion of H_2O_2 being converted into free hydroxyl groups) than any of the heterogeneous catalysts ever reported for the Fenton reaction.[4,17,18]

Experimental Section

Materials: Hydrogen peroxide solution in water (30%, v/v), phenol (≥99% purity), hydrochloric acid (37%, ACS reagent), DMSO (≥ 99.9% purity), and sodium hydroxide (ACS reagent) were supplied by Sigma–Aldrich. Milli-Q water was used in all the experiments. The other reagents used were of analytical or HPLC grade.

Catalysts preparation

Fenton treatment of commercial diamond nanoparticles: Raw diamond nanopowder (1 g) commercially available from Aldrich (ref: 636444, 95+%) was suspended in distilled water (50 mL) in a 500 mL open flask and mixed directly with $FeSO_4{\cdot}7H_2O$ (20 g) as a source of Fe^{2+}. After complete dissolution of the ferrous salt, concentrated sulfuric acid (30 mL) was added to the slurry and the corresponding volume of H_2O_2 (30 wt.% in H_2O) (20 mL) was slowly dropped while observing gases evolution (caution: the Fenton reaction is highly exothermic and occurs with evolution of heat and gases). The process must be carried out cautiously in a well-ventilated fume hood whilst wearing goggles and appropriate personal safety items). This slurry was sonicated on an ice-refrigerated ultrasound bath and held at 1–5 °C for 5 h. Within the first 30 min, the solution turned green/yellow, indicative of iron oxidation. After 1 h, additional amounts of H_2SO_4 and H_2O_2 were added while the suspension becomes yellowish. This second cycle consisting of addition of reagents and sonication was repeated a third time, allowing the final cycle to occur for longer times to ensure the complete decomposition of H_2O_2.

After the Fenton treatment, the suspensions were diluted with distilled water and allowed to reach room temperature. The excess of acid was removed by performing five consecutive centrifugation–redispersion cycles with Milli-Q water. The diamond nanoparticles sediment at the bottom of the centrifuge tube under these conditions. The pH value of the supernatant at the fifth centrifugation–redispersion cycle was neutral. Finally, the Fenton-treated diamond nanoparticles were submitted to overnight freeze-drying to give dry purified diamond nanoparticles (D) as a brownish dust-like material.

Preparation of Au/D catalyst: Au was deposited on Fenton-treated Ds from a solution of $HAuCl_4{\cdot}3H_2O$ (800 mg) in deionized water (160 mL) at three different pH values namely 5, 7.5, and 10. pH adjustment was carried out by addition of NaOH (0.1 M) or HCl (0.1 M) aqueous solutions. Once the pH value was stable, the solution was added to a stirred suspension of D in water. At this moment the slurry was continuously stirred vigorously for 48 h at room temperature and in the dark while monitoring and maintaining the pH if necessary. Au/D was then dispersed in distilled water. The excess of $HAuCl_4$ was removed performing five consecutive centrifugation–redispersion cycles with Milli-Q water. The diamond nanoparticles containing gold sediment at the bottom of the centrifuge tube under these conditions. The pH value of the supernatant at the fifth centrifugation–redispersion cycle was neutral and no traces of chlorides were detected by the $AgNO_3$ test. After removal of the supernatant the catalysts were dried under vacuum at room temperature for 1 h. Then 150 mg of the supported gold catalysts were submitted to three different reduction methods consisting in the thermal treatment with hydrogen (method a), 1-phenylethanol reduction (method b), and $NaBH_4$ reduction (method c). Method a consisting of thermal treatment with H_2 was carried out by placing 150 mg of Au/D catalyst in a quartz reactor and performing the reduction under a hydrogen atmosphere at 300 °C (heating rate: 10 °C min^{-1}) for 6 h. Method b was the 1-phenylethanol reduction of Au/D and was carried out by adding 200 mg of the solid over 30 g of 1-phenylethanol at 160 °C and the mixture was allowed to react over 3 h. Then the catalyst was dispersed in acetone and washed by performing five consecutive centrifugation–redispersion cycles with acetone and a final wash by using Milli-Q water. Finally, the Au/D catalyst was freeze-dried. Method c was based on borohydride reduction of Au and was carried out by suspending 100 mg of Au/D catalyst in aqueous solution (50 mL) with vigorous stirring. Then 5 mL of a 0.1 M fresh solution of $NaBH_4$ was added. After 15 min, the catalyst was washed by performing five consecutive centrifugation–redispersion cycles by using Milli-Q water. Finally, the catalyst suspension was freeze-dried.

The total Au content of the final Au/D catalysts was determined by chemical analysis as follows: 10 mg of the reduced catalyst was placed in a round-bottomed flask (50 mL), connected to a condenser, and 10 mL of *aqua regia* was added under continuous stirring. Then, the temperature was set at 60 °C and the suspension was stirred for 48 h. After this moment, the suspension was filtered through a 0.2 μm Nylon filter and the total gold content of the solution determined by chemical analysis by inductively coupled plasma atomic emission spectroscopy (ICP-AES).

The Au/D catalysts were stored in the dark or used immediately after preparation.

Catalytic tests: Milli-Q water (100 mL) containing phenol (100 mg L^{-1}, 1.06 mM) was placed in a round-bottomed flask. Catalyst (10 mg) was introduced and magnetically stirred. Then, the initial pH was adjusted to the required initial pH value by using HCl (0.1 M) or NaOH (0.1 M). Finally, 200 mg L^{-1} H_2O_2 (30%, v/v) was added to the flask. The pH was continuously monitored and maintained at the required value.

A flow (1 mL min^{-1}) of pure oxygen or nitrogen, when necessary, was bubbled through the phenol solution at the corresponding initial pH and containing the catalyst at least for 45 min prior to the reaction. At this time, the desired amount of H_2O_2 was added. Then, a balloon containing of O_2 or N_2 was placed on the top of flask through a septum to maintain the required atmosphere. At this time the desired amount of H_2O_2 was added.

Productivity test: The productivity test by using Au/D (5H) (see nomenclature in Table 1) was performed by dissolving phenol (5 g) in Milli-Q water (66.7 mL) to which H_2O_2 (33.3 mL, 30%) was added. The solution was magnetically stirred in an Erlenmeyer flask in the dark and then Au/D (5H) (5 mg, 0.99 wt.% of Au) was added. The phenol and H_2O_2 concentration were determined by following the procedure described below but the 100 μL aliquot from the reaction mixture was diluted to 2000-fold in the case of phenol and 5000-fold for H_2O_2.

The reaction pH was continuously monitored and automatically controlled by using a standard 0.01 M solution of NaOH. The reaction time was prolonged over 3.6 days until complete deactivation of the catalyst was observed.

Once the reaction stops due to deactivation of the catalyst, the Au/D (5H) sample was recovered by filtration through a 0.2 μm Nylon filter and washed exhaustively with a basic NaOH aqueous solution (pH 10) and subsequently with Milli-Q water. Then, the solid was dried and used

for a second run. Regeneration of the catalyst was done a second and a third time and, therefore, four uses of the same material under the above conditions were carried out. In the case of the productivity test, the 100 μL aliquot was diluted 2000 times before HPLC analysis.

Phenol and H_2O_2 measurements: Phenol was analyzed by reverse-phase chromatography by using a Kromasil-C18 column as a stationary phase and H_2O/MeOH/CH_3COOH 69:30:1 as the eluent under isocratic conditions and with a UV detector (monitoring wavelength 254 nm). Prior to analysis, aliquots of 2 mL were filtered through 0.2 μm Nylon filters.

The residual H_2O_2 was determined by 10-fold (or 5,000-fold in the productivity test) dilution of the reaction mixture aliquots and by using $K_2(TiO)(C_2O_4)_2$ (Aldrich) in H_2SO_4/HNO_3 as the colorimetric titrator. The solution was allowed to react for 10 min before monitoring at 420 nm.

Quenching and EPR spin-trapping experiments: HO$^\bullet$ radical scavenging experiments were performed by using DMSO. Quenching experiments were carried out under the following conditions: phenol (100 mg L^{-1}, 1.06 mM), H_2O_2 (200 mg L^{-1}, 5.88 mM), air atmosphere, pH 4, Au/D (5H) (100 mg L^{-1}), DMSO to H_2O_2 molar ratio 10 and 8 h reaction time.

The same conditions as above but in the absence of phenol and in the presence of *N-tert*-butyl-α-phenylnitrone (PBN) (1:1 molar ratio to respect H_2O_2) were used to record the EPR spectra of the adduct of PBN and HO$^\bullet$ radicals. EPR spectra were recorded by using a Bruker EMX, with the following settings: frequency 9.803 GHz, sweep width 3489.9 G, time constant 40.95 ms, modulation frequency 100 kHz, modulation width 1 G, microwave power 19.92 mW.

Leaching measurements: The presence of soluble gold species was determined by chemical analysis of filtered solutions. For all the reactions tested, the suspensions were filtered through a 0.2 μm Nylon filter and the liquid phase analyzed by ICP-AES. The detection limit of the technique was 0.1 μg L^{-1}.

Spectroscopic methods: FTIR spectra were recorded on a Nicolet 710 FTIR spectrophotometer by using KBr disks or self-supported wafers compressed to 10 Ton for 2 min.

Diffuse reflectance optical spectra were recorded with a CARY 5G UV/Vis-NIR spectrophotometer containing an integrating sphere.

XRD diffractograms were recorded by using a Philips X'Pert diffractometer equipped with a graphite monochromator, operating at 40 kV and 45 mA and employing Ni filtered $Cu_{K\alpha}$ radiation ($\lambda = 0.1542$ nm).

TEM analysis: The size distribution of the gold nanoparticles was determined by TEM using high angle annular dark field-scanning transmission electron microscopy (HAADF-STEM). The images were obtained by using a FEG-JEOL2010 microscope operated at 200 kV and with a 0.5 nm probe. This technique allows us to identify the gold nanoparticles univocally on the support. To obtain representative particle size distributions of the samples, over 500 particles were counted by using a series of images recorded with the same magnification (800,000). The same equipment was used to obtain high resolution electron microscopy images. Elemental analyses were conducted by combining the STEM mode with X-EDS detectors (Oxford Inca Energy-200).

The fraction of gold atoms on the surface has been estimated by combining HREM modeling and the particle size distribution obtained by HAADF-STEM images. According to HREM images (Figure 1), gold nanoparticles can be considered as exhibiting truncated cuboctahedron morphology. The number of gold atoms on the surface (N_S) and the total amount of gold atoms (N_T) has been obtained by using those models. Then, the percentage of surface gold atoms (D) was calculated according to the following equation:

$$D = \frac{\sum_{i=1}^{i=n} (N_S)_i}{\sum_{i=1}^{i=n} (N_T)_i} \times 100 \quad (4)$$

Acknowledgements

Financial support by the Spanish MICINN (H.G., CTQ2009–11583 and CONSOLIDER-INGENIO Multicat, M.A., CTQ2010–18671, and J.J.C. MAT2008–00889-NAN) is gratefully acknowledged. R.M. thanks the Spanish MICINN for a postgraduate scholarship. S.N. thanks the Technical University of Valencia for a postgraduate research contract (Cantera Programme).

[1] H. J. H. Fenton, *J. Chem. Soc. Trans.* **1894**, *65*, 899.
[2] F. Haber, J. Weiss, *Naturwissenschaften* **1932**, *20*, 948.
[3] J. J. Pignatello, E. Oliveros, A. Mackay, *Crit. Rev. Environ. Sci. Technol.* **2006**, *36*, 1.
[4] S. Navalon, M. Alvaro, H. Garcia, *Appl. Catal. B* **2010**, *99*, 1.
[5] Y. F. Han, N. Phonthammachai, K. Ramesh, Z. Zhong, T. White, *Environ. Sci. Technol.* **2008**, *42*, 908.
[6] S. Navalon, R. Martin, M. Alvaro, H. Garcia, *Angew. Chem.* **2010**, *122*, 8581; *Angew. Chem. Int. Ed.* **2010**, *49*, 8403.
[7] P. W. Chen, Y. S. Ding, Q. Chen, F. L. Huang, S. R. Yun, *Diamond Rel. Mater.* **2000**, *9*, 1722.
[8] M. Haruta, N. Yamada, T. Kobayashi, S. Iijima, *J. Catal.* **1989**, *115*, 301.
[9] S. Navalon, R. Martin, M. Alvaro, H. Garcia, *ChemSusChem* **2011**, *4*, 650.
[10] M. Haruta, *Catal. Today* **1997**, *36*, 153.
[11] A. Corma, H. Garcia, *Chem. Soc. Rev.* **2008**, *37*, 2096.
[12] A. Abad, A. Corma, H. Garcia, *Chem. Eur. J.* **2008**, *14*, 212.
[13] R. Martín, P. C. Heydorn, M. Alvaro, H. Garcia, *Chem. Mater.* **2009**, *21*, 4505.
[14] R. Martín, M. Alvaro, J. R. Herance, H. Garcia, *ACS Nano* **2010**, *4*, 65.
[15] R. Martín, S. Navalon, M. Alvaro, H. Garcia, *Appl. Catal. B* **2011**, *103*, 246.
[16] M. J. Burkitt, R. P. Mason, *Proc. Natl. Acad. Sci. USA* **1991**, *88*, 8440.
[17] L. F. Liotta, M. Gruttadauria, G. D. Carlo, G. Perrini, V. Librandod, *J. Hazard. Mater.* **2009**, *162*, 588.
[18] E. G. Garrido-Ramírez, B. K. G. Theng, M. L. Mora, *Appl. Clay Sci.* **2010**, *47*, 182.

Received: March 28, 2011
Revised: May 3, 2011
Published online: July 15, 2011

